Journal of Optoelectronics and Advanced Materials Vol. 5, No. 2, June 2003, p. 421- 427

STRUCTURE-PROPERTIES RELATIONSHIPS IN ELECTRODEPOSITED Ni-W THIN FILMS WITH COLUMNAR NANOCRYSTALLITES

N. Suliţanu*, F. Brînzã

Department of Solid State Physics, Faculty of Physics, "Al. I. Cuza" University, 6600 Iasi, Romania

Ni-W thin films with columnar nanocrystallites have been prepared by electrodeposition. Samples containing from zero to 18 wt. % W and 140 nm in thickness have been selected for measurements. Perpendicular magnetic anisotropy (PMA) was clearly observed in films with tungsten content of about 13 wt. %. Typical films of this composition consisted of columnar nanocrystallites of about 12.5 nm size in diameter embedded in an amorphous Ni-W matrix. This segregated mixed structure, i.e., two-phase heterogeneous alloy film, resulted in the large PMA energy constant $K_{\perp}$ of 120 kJ/m^3 and in the high perpendicular coercivity $H_{c\perp}$ of 120 kA/m. Also, these two-phase Ni-W thin films exhibited sufficiently high saturation magnetization M_s of 420 kA/m. It is concluded that electrodeposited Ni-W typical thin film (13 wt. % W) may be applicable for the media in the perpendicular magnetic recording system.

(Received January 27, 2003; accepted May 8, 2003)

Keywords: Nickel-tungsten alloy, Electrodeposition, Nanocrystalline thin films, Coercivity, Perpendicular magnetic anisotropy

1. Introduction

In the last years a great variety of nanostructured magnetic materials have been prepared because of their unusual physical properties compared to bulk materials. They may have numerous applications in industry and also in magnetic recording media, sensors and other devices [1-5]. Many different techniques have been employed to produce nanostructured materials [6]. Among them, electrodeposition of nanostructured metal films has many advantages. It can be carried out at ambient temperature and pressure, and therefore requires much less complex apparatus than vacuum-based techniques such as sputtering and molecular beam epitaxy. Electrodeposition offers real advantages to automatically prepare identical films, onto large substrates, with a great variety of microstructure, and hence various property. Also, electrodeposition can be used to fabricate metal and metal-oxide nanostructures with a wide variety of interesting and potentially useful electronic properties [7-9]. Nevertheless, many improving must to bring so that the film surface to be sufficiently smooth (surface roughness of less than 1 nm is required for both longitudinal and perpendicular recording configurations) and to prevent the surface corrosion effects. The study of electrodeposited nanostructures is still at a very early stage, but the combination of electrochemistry and patterning on the nanometer scale seems highly likely to lead to further exciting developments [10,11].

The mean goal of our research was to prepare by electrodeposition and magnetically characterize nanocrystalline Ni-W alloy films. Tungsten forms hard alloys with iron group metals especially with nickel and cobalt, retaining some of its unusual magnetic, electrochemical and mechanical properties, even at elevated temperature, and also exhibiting good corrosion resistance towards acidic and alkaline media [12,13]. In the case of Ni-W alloy films, the combination of useful

* Corresponding author: sulitanu@uaic.ro

Ni magnetic properties with excellent W wear resistance is of special interest, wear being a major problem in the utilization of thin films [1-4]. Nickel and tungsten are insoluble in the solid and liquid phase because of the high difference in diameter, higher than 15 % [12]. For this reason, it is expected that a great variety of non-equilibrium (metastable) structural phases, and hence properties, to be formed at alloying of these chemical elements.

This paper reports on structural and magnetic characterization of face-centred cubic (fcc) Ni-W nanocrystalline alloy films prepared by electrodeposition. Nickel is ready electrodeposited from aqueous solutions as pure metal or even quaternary alloys. Opposite to nickel, tungsten does not deposit from aqueous solutions as pure metal. Therefore, by co-deposition of these two metals it is expected to obtain interesting magnetic structures. In a previous paper [14] we presented the first attempt for obtaining and characterization of Ni-W alloy films. In this paper we focussed on the electrodeposition procedure of nanostructured Ni-W alloy films and their structural and magnetic characterization. Columnar crystallites were found to be a prominent structure characteristic in these films. We, also, reveal the presence of perpendicular magnetic anisotropy in nanostructured Ni-W films, mainly determined by the addition of tungsten into the Ni film.

2. Experimental

The Ni-W films were deposited at a constant current density using a dc highly stabilized source. We have started from a sulphate bath with the same composition as in previous work [14] whose deposition parameters were strongly modified so that the conditions for the nanocrystal formation to be provide: high nucleation rate (over potential phenomena) and slow crystallite growth (adsorption/desorption processes of inhibiting molecules). The relevant experimental parameters those it was paid more attention were the physical parameters (bath temperature, hydrodynamic electrolyte conditions, current density, deposition time) and chemical parameters (pH value, addition of complex formers or inhibitors). Therefore, high pure preparation conditions equivalent to ultrahigh-vacuum of approximately 10^{-10} mbar were used which allowed the reproducible deposition of Ni-W films [15]. The plating cell de-aeration was achieved by *in situ* saturation of the electrolyte with pure Ar gas. During alloy film preparation the plating cell was tightly capped in order to minimize the effect of air inflow. A self-valve mounted in the body cap allowed the electrolysis gas evacuation. The plating cell was thermostatically controlled in the temperature range 306 ± 0.5 K. The pH of the plating bath was fixed at either 2.0 using a 35 % NH_4OH solution and was controlled by means of the electronically operated pH-meter. While the electrolyte was being stirred (30-60 cycle/min) the dc current density reached an optimal value of 300-600 A/m^2, depending on W^{2+} ions concentration in electrolyte solution. These physical and chemical electrodeposition conditions give us the possibility that to intentionally adjust the film microstructure (crystallite size, distribution and shape, microstress) which in the last determines the physical and chemical film properties (conductivity, magnetism, chemical stability, hardness). The plating bath contained as a base electrolyte nickel sulphate, boric acid, sodium and potassium ditartrate, sodium citrate and, respectively, sodium tungstate [14,15]. Moreover, in contrast to the previous electrolyte [14], 0-7 mol m^{-3} of cumarine was added in order to avoid dendritic deposition [16]. The Ni anode and copper cathode (substrate), situated at a distance of 3 cm, was disc-shaped and films with 1.8 cm in diameter were obtained.

The film thickness, D, currently ranging from 120-150 nm, was interferometrically measured [17]. The tungsten content in the films, maximum 18 wt. %, was determined by electron probe microanalysis (EPMA). The films were investigated by X-ray diffraction (XRD) with Mo Kα radiation (λ = 0.0709 nm) using a standard θ-2θ diffractometer and, also, by scanning (SEM) and transmission (TEM) electron microscopy. The films were scanned in air with atomic force microscope (AFM) with a resolution of 512×512 pixels. The average nanocrystallite size was estimated by using the Scherrer's equation modified by Warren and Biscoe [18], $d = (0.94\lambda)/(\beta\cos\theta)$, where d is the average crystallite size in nm (the coherent scattering length), λ is the radiation wavelength, β is the corrected half-width at half intensity (in radius), and θ is the diffraction peak angle. The Ni crystallite size and in some cases crystallite size distribution, as well as Ni crystallite morphology were directly evaluated from SEM, TEM micrographs and AFM images. The saturation magnetization and effective perpendicular anisotropy of films were measured with an automatic torque-magnetometer (ATQM) in

dc fields up to 480 kA/m, at room temperature [19]. The in-plane and transversal to plane film hysteresis properties were measured by using a vibrating sample magnetometer (VSM) in dc fields up to 720 kA/m, at room temperature.

3. Results and discussion

X-ray diffractometry clarified that the electrodeposited Ni-W films consisted of very fine fcc Ni crystallites whose (111) axes are preferentially oriented in the direction perpendicular to the film plane. Fig. 1 shows XRD patterns for a pure Ni film and for three Ni-W films containing 6, 14 and, respectively, 18 wt. % W. The XRD patterns of all films indicate a peak from the (111) planes and very weak peaks from the (220), (222) and (331) planes only for pure Ni film. Therefore, the nickel crystallites have mainly the preferred crystallographic growth orientation [111]. This suggests that the nickel atom diffusivity in the direction normal to the substrate was different from that parallel to the substrate. This means that there is the anisotropy of surface diffusion, i.e., moving atoms on the surface has a tendency to ascend crystallites rather than to descend crystallites (the Schwoebel effect [20]). The (111) peak intensity monotonically decreases while its width increases with the increase of W content in the Ni film. This suggests the refinement of the grains. Moreover, XRD patterns clarified that the Ni-W electrodeposited films with W content below 6 wt. % are composed of fcc Ni crystallites whose [111] axes are preferentially oriented in the direction perpendicular to the film plane. This kind of films was denominated as single-phase Ni films although the interfaces between crystallites are present, namely W enriched crystallite boundaries. It can be observe on Fig.1 that the diffraction peak corresponding to fcc (111) Ni steeply decreases in intensity, broadens and monotonically shifts to the side of the lower diffraction angle 2θ with W content increase over 6 wt. %. This means that the spacing between the adjacent Ni (111) planes was expended due to the large internal stress resulting from high number of W atoms segregated at the boundaries of very fine Ni crystallites. These films belong to a transition structural region from fcc nanocrystalline phase to amorphous phase. Therefore, depending on film composition, two types of nanostructures were observed: (a) single-phase nanostructure (< 6 wt. % W) which consist of Ni crystalline cores-nanocrystallites (highly magnetic phase) separated by interfaces or "interphases", namely W enriched crystallite boundaries (14-27 nm), and (b) two-phase nanostructure (6-18 wt. %) in which a second Ni-W amorphous phase or even amorphous-disordered mixture separates the magnetic Ni nanocrystallites (6-14 nm).

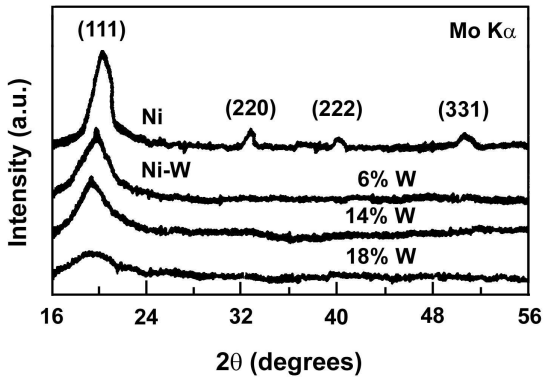

Fig. 1. X-ray diffraction patterns of nanostructured films as a function of W content: for a pure Ni film and for Ni-W films with 6, 14 (*typical film*) and, respectively, 18 wt % W.

Fig. 2a shows TEM micrograph for a *typical Ni-W film* which contains *14 wt. % W* in composition. TEM micrograph reveals that the Ni-W film consists of a Ni-W amorphous matrix and single or here and there agglomerated Ni crystallites. The particles are quite equiaxial in circular shape, having sizes in the nanometer range with a rather narrow size distribution. Fig. 2b shows SEM image of cross section of *typical Ni-W film*. SEM image indicate that electrodeposited two-phase

Ni-W film is in fact of nanofibrous structure. The nanofibres grow perpendicularly to the copper support and here and there group into well packed bundles. The AFM image of *typical Ni-W film* surface, *14 wt. % W*, is shown in Fig. 2c. The surface morphology appears to be a set of continuous columnar (fibrous) crystallites. The average diameter of the columnar (fibrous) crystallites determined from SEM and AFM micrographs equals 13 nm and this value is in well agreement with average size of 12.5 nm estimated by using the Scherrer's equation [18]. Since the films have particulate structure, there is a close correlation between the (111) film texture and the crystallite columnar shape [21]. The crystallites isolation is low in single-phase films (< 6 wt. % W), i.e., only by boundary interphase, but is sufficiently high in two-phase films (> 6 wt. % W) when a large volume fraction of mixed Ni-W, amorphous or highly disordered, phase appeared in the film.

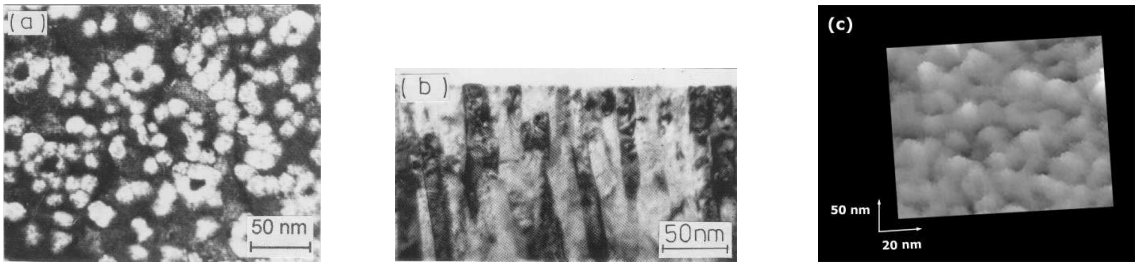

Fig. 2. TEM micrograph (a), SEM cross section micrograph (b) and AFM image (c) for a *typical nanostructured film* with 14 wt. % W in composition. The AFM image size is 100×80 nm.

Therefore, the nanocrystalline-amorphous Ni-W films (7-18 wt. % W) behave as an assembly of Ni columnar nanocrystallites (6-14 nm) embedded in a weak-magnetic Ni-W metallic matrix.

Fig. 3 shows the change of crystallite size, d and saturation magnetization, M_s as a function of W content in nanocrystalline Ni-W thin films.

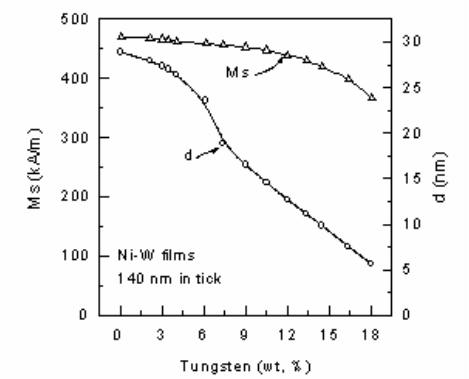

Fig. 3. The diameter average size of Ni columnar crystallites, d and saturation magnetization, M_s for Ni-W thin films as a function of tungsten content.

The crystallite size decreases non-linearly and displays a kink for approximately 6 wt. % W, which corresponds to the beginning of amorphous phase development in the film. For films in which the amorphous phase is present, the crystallite size, d, decreases linearly. The amorphous volume fraction of the intercrystallites region increased with the tungsten content increase while the crystallite size decreased. As a consequence, by varying the crystalline/amorphous ratio through W content change, the relative volume fraction of the crystallites and the size of consolidated crystallites in Ni-W thin film can be manipulated. For a pure Ni film with 29 nm crystallite size was found M_s = 482 kA/m. When the crystallite size decreases M_s also decreases reaching a minimum of about

350 kA/m for a Ni-W film with columnar crystallites of 6 nm in diameter. The weak ferromagnetism of the mixed phase correlated with long-range magnetic interaction between the crystallites contributes to the low saturation magnetization of the nanocrystalline Ni-W films. The reduction of magnetization in the smaller crystallites has been also attributed mainly to the surface-interface effects on the crystallite boundary [22]. The boundary region differs structurally as well as chemically from the crystallite core because the W atoms preferentially segregated at the crystallite surface. As a result, magnetic properties in the boundary region strongly differ in comparison with the crystallite core. For a *typical Ni-W film, 14 wt.% W,* with columnar crystallites of 12.5 nm in diameter it was found M_s = 420 kA/m.

Fig. 4 shows the in-film plane and transversal-to-film plane magnetization curves (hysteresis loops) for three Ni-W thin films with different W content, i.e.: 6, 14 (*typical Ni-W film*) and 18 wt. %.

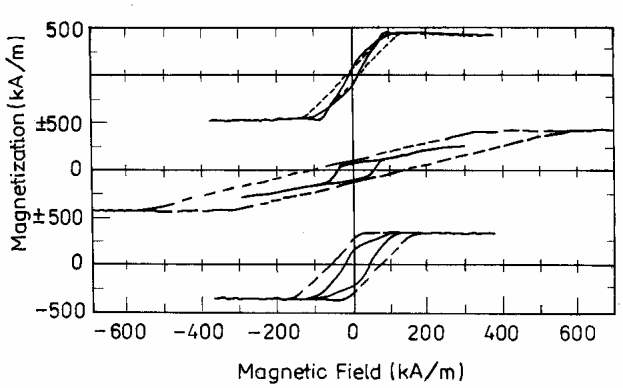

Fig. 4. Magnetization curves (hysteresis loops) measured while applying the in-film plane and, respectively, transversal-to-film plane magnetic field: (a) 6 wt. % W; (b) 14 wt. % W (*typical Ni-W film*); (c) 18 wt. % W.

The in-plane magnetization curves have almost the same shape, i.e., the hysteresis loops undergo a small rapid change near the coercive field, $H_{c//}$, and a gradual (linear) change up to magnetization saturation. The higher rate of rapid change near $H_{c//}$ is reached for *typical Ni-W film* when hysteresis loop clear has a rhomboidal shape. In the case of transversal-to-plane magnetization curves, since the magnetic field is applied perpendicular to the film plane, the influence of the demagnetizing field, $H_d = - N_\perp M_s = - M_s$ (the demagnetizing factor, $N_\perp = 1$ for thin films), must be considered. Shearing correction has been carried out for these kinds of curves (Fig. 4) by subtracting H_d from the applied magnetic field. All transversal-to-plane hysteresis loops are rhomboidal. When the magnetic field decreases from saturation magnetization state, a rapid change appears at the beginning of the magnetization reversal region and then magnetization decreases almost linearly.

The saturation magnetization, anisotropy field, H_k and perpendicular magnetic anisotropy (PMA) energy, $K_\perp$ for each of three Ni-W films are summarized in Table 1. Also, the in-plane, $H_{c//}$ and transversal-to-plane, $H_{c\perp}$ corcivities of the films are given in Table 1.

Table 1. Magnetic properties of Ni-W films for different tungsten content from in-plane and transversal-to-plane magnetization curves and torque-magnetometry measurements.

Tungsten wt. %	M_s kA/m	$H_{c//}$ kA/m	$H_{c\perp}$ kA/m	H_k kA/m	$K_\perp$ kJ/m^3
6	460	12.5	20	107	30
13*	420	50	120	455	120
18	350	32	69	91	20

* *Typical Ni-W films* so were denominated in the work presentation

The transversal-to-plane hysteresis loop for *typical Ni-W film, 14 wt. % W*, shown in Fig. 4b is quite similar to that of films which exhibit PMA with stripe domain structure and magnetic reversal by magnetic wall displacement [23-25]. Therefore, it is estimated to have PMA in typical Ni-W film. This is supported by the fact that the field strength of saturation in the in-plane magnetization curve is higher than that in the transversal-to-plane magnetization curve and $H_{c\perp}$ is larger than $H_{c//}$. For this typical film $H_{c\perp}$ is twice that of others. The PMA energy, $K_\perp$ = 120 kJ/m^3, saturation magnetization M_s = 420 kA/m and perpendicular coercivity $H_{c\perp}$ = 120 kA/m are almost equal to those of Co-Cr thin films [26]. The squareness ratio, $S = M_r/M_s$ (M_r is remanent magnetization) of the in-plane M-H hysteresis loop was as low as 0.2. These results indicate that there are regions with strong uniaxial anisotropy in the direction perpendicular to the film plane. The origin of this large PMA in Ni-W typical films is mainly attributed to the magnetoelastic anisotropy associated with in-plane internal stress and positive magnetostriction [27]. The secondary source of PMA is believed to be the magnetocristalline anisotropy of <111> columnar crystallites and its shape magnetic anisotropy [27, 28]. The enhanced coercivity must be the result of the high uniaxial magnetic anisotropy of the isolated columnar Ni crystallites [27, 29]. The large $K_\perp$ and high $H_{c\perp}$ are sufficient to apply these alloy thin films to the perpendicular magnetic recording [30]. The low temperature of the electrodeposition (306 K) is also an advantage for deposition of Ni-W thin films on polymer tape substrates such as polyethylene terephtalate (PET) and polyethylene naphtalate (PEN), of which the glass transition temperatures are about 343 and 393 K, respectively, for production of flexible media such as floppy disks and recording tape. The large values of $H_{c\perp}$ and $K_\perp$ obtained for typical Ni-W film has not been attained in the sputtered Co-Cr thin film deposited at substrate temperature as low as such a temperature. It is concluded that the electrodeposited Ni-W thin films can be one of the perpendicular magnetic recording media prepared at a low-temperature process and uniform onto large substrates.

4. Conclusions

Ni-W electrodeposited thin films with W content of about 14 wt % consisted of fine columnar crystallites, d = 12.5 nm and exhibited large perpendicular magnetic anisotropy (PMA). Such Ni-W typical films are characterized by the fowling magnetic parameters: relatively high saturation magnetization, M_s = 420 kA/m, sufficiently large perpendicular coercivity, $H_{c\perp}$ = 120 kA/m and large $K_\perp$ = 120 kJ/m^3. From this point of view, the Ni-W films with PMA had a critical composition for which it was established an equilibrium between magnetocrystalline anisotropy energy of <111> columnar crystallites and magnetoelastic energy of the in–plane internal stress whatever their nature was. We consider that the appearance and development of the interface between magnetic crystalline core (Ni) and weak–magnetic boundary layer (Ni–W) for films with W content higher than 6 wt. % is the driving mechanism of perpendicular magnetic anisotropy (PMA) arising. It is considered that Ni-W films with such a large $K_\perp$ associated with relatively high saturation magnetization should be used as alternative media for ultrahigh density perpendicular magnetic recording.

Acknowledgements

The author would like to thanks Prof. dr. Gh. Popa and Drd. N. Apetroaiei, Physics Faculty of Iasi for his help in AFM investigations and, also, Dr. M. Taşcă, Technical University of Iaşi for their help in SEM & TEM investigations. This research is founded in part by the MEC-CNCSIS.

References

[1] C. D. Mee, E. D. Daniel, Eds., Magnetic Recording Technology, IEEE Press, New York (1997).
[2] Y. Nakamura, in: Magnetic Storage Systems Beyond 2000, Ed. G.C. Hadjipanayis, Kluwer Academic Press, NATO Sciences Series vol. 41, Dordrecht 75-102 (2001).
[3] K. Ouchi, N. Honda, IEEE Trans. Magn. **36,** 16-22 (2000).
[4] P. Ciureanu, S. Middelhoek, Thin Film Resistive Sensors, IOP Publishing, London (1992).

[5] K. O`Grady, H. Laidler, J. Magn. Magn. Mater. **200,** 616-633 (1999).
[6] F. J. Himpsel, I. E. Ortega, G. I. Mankey, R. F. Willis, Adv. Phys. **47,** 511-597 (1998).
[7] I. Kazeminezhad, H. J. Blythe, W. Schwarzacher, Appl. Phys. Lett. **78,** 1014-1017 (2001).
[8] T. Osaka, Electrochem. Acta **45,** 3311-3321 (2000).
[9] E. Tóth-Kádár, L. Péter, T. Becsei, J. Tóth, L. Pogány, T. Tarnóczi, P. Kamasa, I. Bakonyi, G. Láng, A. Cziráki, W. Schwarzacher, J. Electrochem. Soc. **147,** 3311-3318 (2000).
[10] I. Tabakovic, V. Inturi, S. Riemer, J. Electrochem. Soc. **149,** C18-C22 (2002).
[11] W. Schindler, D. Hofman, J. Kirschner, J. Appl. Phys. **87,** 7007-7009 (2000).
[12] W. Hume-Rothery, G. V. Rainor, The Structure of Metals and Alloys, The Institute of Metals, London (1962) p. 250.
[13] C. L. Aravinda, V. S. Muralidharan, S. M. Mayanna, J. Appl. Electrochem. **30,** 601-606 (2000).
[14] N. Sulitanu, Mater. Lett. **14,** 295-297 (1992).
[15] N. Sulitanu, in: Synthesis, Functional Properties and Applications of Nanostructures, Eds. T. Tsakalakos, I. A. Ovid'ko, Kluwer Academic Publishers, Dordrecht (2002) in press.
[16] N. Sulitanu, F. Brînză, J. Optoelectron. Adv. Mater. **4 (2),** 285-288 (2002).
[17] W. A. Pliskin, S. J. Zanin, in: Handbook of Thin Film Technology, Vol. 2, Eds. L.I. Maissel and R. Glang, McGraw Hill, New York (1970) p. 176.
[18] H. P. Klug, L. E. Alexander, X-Ray Diffraction Procedures for Polycrystalline and Amorphous Materilas, John Wiley, New York (1974) p. 662.
[19] N. Sulitanu, Rom. Res. Phys. **44,** 699-709 (1992).
[20] R. L. Schwoebel, E. J. Shipsey, J. Appl. Phys **37,** 3682-3686 (1966).
[21] K. Itoh, K. Okamoto, T. Hashimoto, H. Fujiwara, J. Magn. Magn. Mater. **8,** 247-252 (1990).
[22] K. M. Krishnan, Acta Mater. **47,** 4233-4244 (1999).
[23] C. Kooy, U. Enz, Philips Res. Rep. **15,** 7-11 (1960).
[24] D. S. Lo, M. M. Hanson, J. Appl. Phys. **38,** 1342-1343 (1967).
[25] W. Ändra, H. Danan, phys. stat. sol. (a) **42,** 227-233 (1977).
[26] K. Ouchi, IEEE Trans. Magn. **36,** 16-22 (2000).
[27] N. Sulitanu, J. Magn. Magn. Mater. **231,** 85-93 (2001).
[28] L. Callegaro, E. Puppin, IEEE Trans. Magn. **33,** 1007-1011 (1997).
[29] H. Szymczak, J. Magn. Magn. Mater. **200,** 425-438 (1999).
[30] P. J. Grundy, J. Phys. D: Appl. Phys. **31,** 2975-2990 (1998).